Available online at www.sciencedirect.com
SCIENCE DIRECT®
Bioorganic & Medicinal Chemistry Letters 15 (2005) 1737–1741
Bioorganic & Medicinal Chemistry Letters

A two-state homology model of the hERG K^+ channel: application to ligand binding

Ramkumar Rajamani, Brett A. Tounge, Jian Li and Charles H. Reynolds*

Drug Discovery, Johnson & Johnson Pharmaceutical Research & Development, PO Box 776, Welsh and McKean Roads, Spring House, PA 19477-0776, USA

Received 5 October 2004; revised 5 January 2005; accepted 6 January 2005

Abstract—Homology models based on available K^+ channel structures have been used to construct a multiple state representation of the hERG cardiac K^+ channel. These states are used to capture the flexibility of the channel. We show that this flexibility is essential in order to correctly model the binding affinity of a set of diverse ligands. Using this multiple state approach, a binding affinity model was constructed for set of known hERG channel binders. The predicted pIC_{50}s are in good agreement with experiment (RMSD: 0.56 kcal/mol). In addition, these calculations provide structures for the bound ligands that are consistent with published mutation studies. These computed ligand bound complex structures can be used to guide synthesis of analogs with reduced hERG liability.

A K^+ channel expressed by the human ether a go–go related gene (hERG) plays an important role in the normal repolarization of the cardiac action potential. Impairment of this repolarization is associated with cardiac arrhythmia and long QT syndrome (LQTS).[1,2] LQTS has arisen as a serious potential side effect since many known drug molecules bind to the hERG K^+ channel.[3] For example a number of antihypertensives, anticancer agents, antipsychotics, and antihistamines have been shown to have high affinities.[3] Given the large number of drugs that have some affinity for the hERG K^+ channel and the potential seriousness of LQTS, the hERG K^+ channel has become a target of great concern to the pharmaceutical industry.

A detailed structural understanding of the features of the hERG K^+ channel, and how ligands bind to it, would aid medicinal chemists in designing new drugs that have reduced potential for hERG liability. Experimental mutational studies carried out in the Sanguinetti lab have shown that the probable binding site for drug ligands is the cavity under the selectivity filter near the S6 helix.[4–7] These studies identified two key residues Tyr652 and Phe656 and also provided some general understanding of the nature of interactions involved (e.g., cation-π, π–π, and hydrophobic).[8] Computational studies based on docking of ligands into a homology model (derived from KcsA) have been previously reported.[4] In addition, several pharmacophore and QSAR models have been developed that describe key features for hERG K^+ channel binding and predict binding affinities.[9–11] These models provide a useful framework for understanding binding, but are limited in their ability to give structural insight into the specific protein–ligand interactions responsible for affinity and how one might modify any given structure to mitigate binding. In addition, none of the previously derived models have attempted to address the issue of the flexibility of the hERG K^+ channel. It is known from electrophysiology experiments that the channel must be in the active open state for many compounds to bind. In this state the cavity residues identified as important for binding in the mutation studies are accessible. However, once a compound enters the cavity region, the S6 helices can close to varying degrees depending on the bound ligand. Thus, it is unlikely that a single snapshot of the channel state would capture the energetics of binding for a diverse set of ligands. To address this issue we have developed an approach that uses multiple homology models to represent the flexibility of the channel. As a validation of this approach, we use the linear interaction energy (LIE) method to predict the

Keywords: hERG channel; Homology model; Ligand binding; Structure based design.
* Corresponding author. Tel.: +1 215 628 5675; fax: +1 215 628 4985; e-mail: creynol1@prdus.jnj.com

0960-894X/$ - see front matter © 2005 Elsevier Ltd. All rights reserved.
doi:10.1016/j.bmcl.2005.01.008

binding affinity and structure of the ligand–protein complexes for a set of 32 ligands with published IC_{50} values.[9] The list contained IC_{50} values only for hERG K^+ channels expressed in mammalian cells.[9]

Our initial hERG channel homology model was constructed from the closed state crystal structure of KcsA (pdb code 1K4C, Resolution 2 Å).[12] This model was built using the PRIME homology modeling program.[13] First, the sequence of the pore forming region of the channel (S6 helix) was aligned with the KcsA template based on the published sequence alignment.[12] This was followed by extraction of atom coordinates from the template. The crystallographic positions of the backbone atoms and conserved side chains were mapped from the template. The side chain coordinates for all non-identical residues were predicted using PRIME.[13] Inspection of this model revealed that the size of the active site cavity was simply too small to accommodate many of the known ligands for hERG. Sequence comparison revealed that the hERG K^+ channel contains a Phe656 residue in an equivalent position to Thr in KcsA. The difference in size of the two residues may argue for a hERG K^+ channel structure differing in the S6 helix position from that of the closed KcsA structure. For this reason, a homology model was also constructed based on the crystal structure of MthK (pdb code 1LNQ),[14,15] which is representative of the open state of the channel. While the MthK structure is of lower resolution (3 Å), it does provide some insight into the helix movement in going from the open to closed states of the channel. Overlay of the crystal structures of KcsA and MthK reveals a bending of the S6 helix at the glycine hinge between the closed and open states.[15] The direction and angle of this bend between the closed (KcsA) state and the opened (MthK) states were used as reference points to derive a number of intermediate states of the helix motion. The S6 helices of the KcsA based model were translated outwards from the glycine hinge by defining a rotational axis perpendicular to the S6 helical axis. Initially the S6 helix from the reference closed state was rotated in order to match the opened MthK helix position. The side chains of the translated open state were re-predicted using PRIME. The channel was then closed in 1° increments and subjected to a short protocol of heating (0.4 ps), equilibration (0.6 ps), and dynamics (5 ps) using the CHARMM force field.[16,17] A harmonic constraint of 24 kcal/mol/Å^2 was applied on the C_α atoms during this process. This protocol relieved any unfavorable interactions arising from the translation of the helices. Two states were picked for this study, the partially open state represented by a 10° translation away from the KcsA reference state, and the fully open state obtained from a 19° translation. This latter structure closely corresponds to the MthK S6 helix position. Overlay of the states generated from the KcsA model, and the axis of rotation are shown in Figure 1. These two states (homology models) were used for docking the ligand training set.

We used the protein preparation utilities in Maestro[18] to assign the charge state of ionizable residues, add hydrogens, and carry out a highly constrained minimization of the open and partially open ion channel states. The ligand set was prepared for docking using the LigPrep utility to define the charge state and enumerate the stereo isomers for each ligand. The ligand set was then docked into each of the hERG K^+ channel homology models (open, partially open) using GLIDE.[19] A total of 10 poses per ligand (top Glide score poses) were kept for evaluation for each docking run. After docking, the best pose for each ligand (based on the e-model score) was minimized within the protein. This minimization was performed using a conjugate gradient minimizer (0.05 convergence criteria), the OPLS-AA force field, and GB/SA continuum water model.[20–22] Protein residues that fell within 8 Å of the binding site were allowed to optimize during minimization. All other residues were held fixed. Finally, the ligand from the minimized

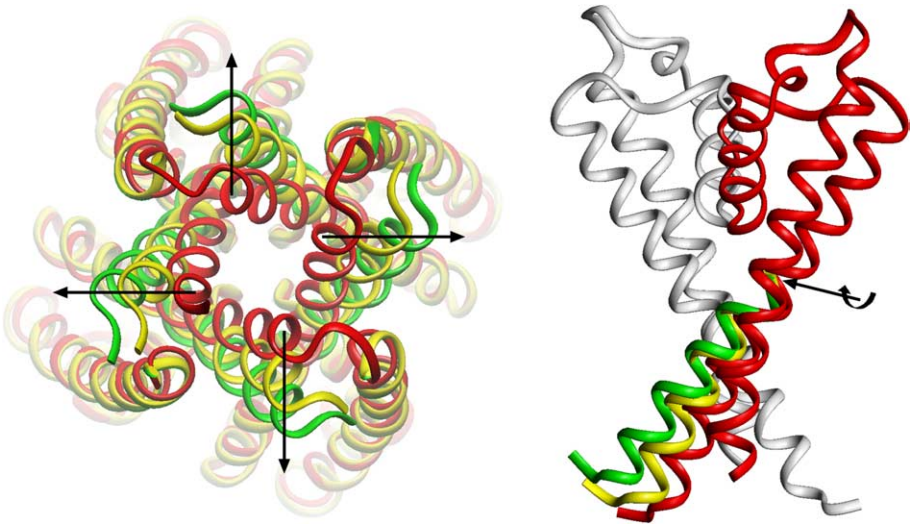

Figure 1. Representation of the direction of rotation and helix twist for channel pore opening. Color scheme: red (closed state derived from the reference KcsA structure), yellow (partially open structure represented by a10° tilt), green (open state represented by 19° tilt).

ligand–receptor complex was extracted and minimized in GB/SA water to obtain reference energetics for the free state. The computed difference in the electrostatic (Δele) and van der Waals (Δvdw) energies between the bound and free states, were used to derive linear regression fits to the experimental pIC_{50}s.

As expected, models derived for the open or partially open states exclusively resulted in very poor fits. An example fit for the model derived for all ligands bound to the partially open state (R^2 0.24) is shown in Figure 2.

As an initial attempt to capture the known flexibility of the cavity helices we looked at a dual state model where the ligands are separated into bins based on their preference for a particular state of the ion channel. In this case we used the homology models for the open and partially open states of the hERG K^+ channel described previously. These states were chosen for the initial model because they represent two extremes of the cavity size. The open state approximates the MthK helix positions and the partially open state allows for enough helix tilt to relax the strain in the Phe656 residues. The preference of a particular ligand for a given state was established by comparing the estimated interaction energy (sum of the Δele and Δvdw terms) for each ligand in both states and picking the state with the lower value. A total of 21 ligands preferred the open state and the remaining 11 ligands preferred the partially open state. A linear regression fit to the Δele and Δvdw terms for ligands in each state was derived using the statistical program S-plus.[23]

For the open state model a RMSD of 1.2 for the computed pIC_{50} was obtained. For the partially open state model, a fit with a pIC_{50} RMSD of 0.85 was obtained. The plots of the predicted versus experimental pIC_{50}s bound to the open and partially open forms are shown in Figures 3 and 4. Eqs. 1 and 2 represent the models obtained for the open and partially open states, respectively.

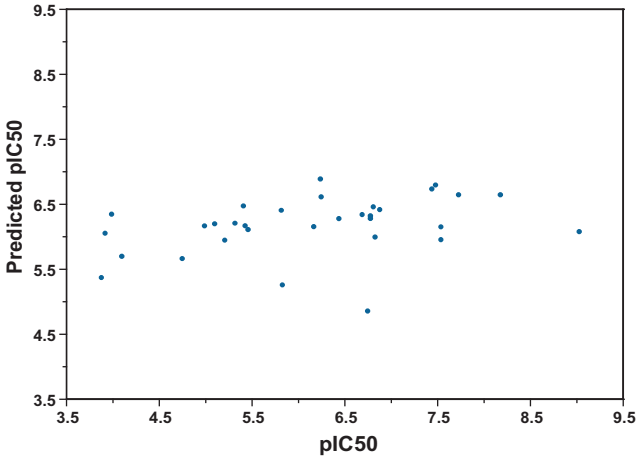

Figure 2. Plot of the experimental versus computed pIC_{50} for the partially open state in a single state model.

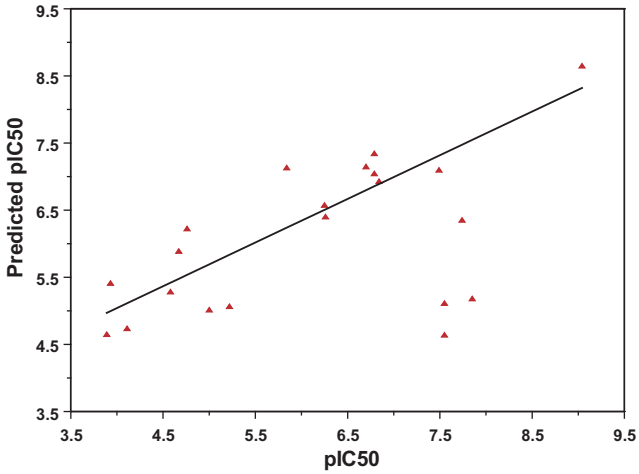

Figure 3. Plot of the experimental versus computed pIC_{50} for the open state. The solid line represents the robust MM fit.

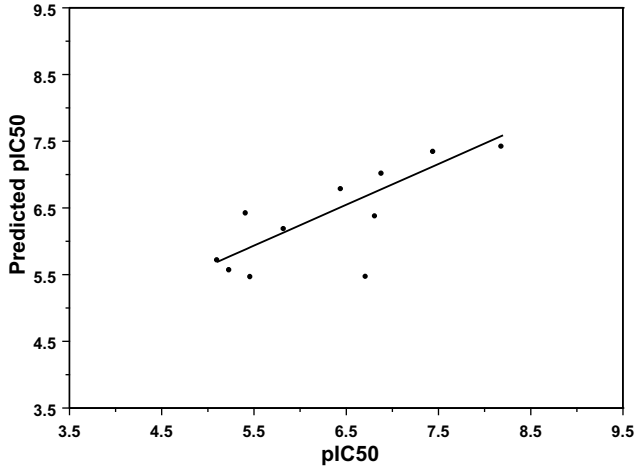

Figure 4. Plot of the experimental versus computed pIC_{50} for the partially open state. The solid line represents the robust MM fit.

It is clear from these fits that allowing the channel to adopt two different states has a significant impact on the ability to model these ligands.

$$pIC_{50_{Open}} = -0.166(\Delta vdw) + 0.002(\Delta ele) \quad (1)$$

$$pIC_{50_{Partially\ open}} = -0.155(\Delta vdw) + 0.0004(\Delta ele) \quad (2)$$

Inspection of Eqs. 1 and 2 reveal essentially equivalent coefficients for the Δvdw term. Given this fact, we replaced Eqs. 1 and 2 with a single model. This model was constructed by combining the energies for each ligand from its best fit state (i.e., open or partially open as determined above). On plotting the experimental versus computed pIC_{50} for this combined model, five ligands (clozapine, haloperidol, norastemizole, and pimozide) were identified as potential outliers. Omitting these five compounds, resulted in a model with an RMSD of 0.56 (R^2 0.82) (Table 1, Eq. 3). Visual inspection of the protein–ligand complex revealed no obvious reason for this outlier status. One possible explanation is

Table 1. Ligands[a] included in the docking studies

Compound	$pIC_{50_{Observed}}$	$pIC_{50_{Predicted}}$	$\Delta pIC_{50_{(Obsd-Pred)}}$
Open state			
Amitriptyline	5.00	4.59	0.41
Astemizole	9.04	8.10	0.94
Azimilde	6.25	6.06	0.19
Bepridil	6.26	5.99	0.27
Diltiazem	4.76	5.80	−1.04
Dolasetron	5.22	4.80	0.42
Domperidone	6.79	7.06	−0.27
Droperidol	7.49	6.67	0.82
Fexofenadine	4.67	5.58	−0.91
Gatifloxacin	3.89	4.21	−0.32
Grepafloxacin	4.11	4.29	−0.18
Halofantrine	6.70	6.89	−0.19
Haloperidol	7.55	5.05	2.50[b]
Mibefradil	5.84	6.68	−0.84
Moxifloxacin	3.93	5.04	−1.11
Norastemizole	7.55	4.65	2.90[b]
Pimozide	7.74	6.29	1.45[b]
Risperidone	6.79	6.77	0.02
Sertindole	7.85	5.15	2.70[b]
Sparfloxacin	4.58	4.82	−0.24
Verapamil	6.84	6.64	0.20
Partially open state			
Chlorpromazine	5.83	5.75	0.08
Cisapride	8.19	7.36	0.83
Clozapine	6.72	5.47	1.25[b]
Cocaine	5.24	5.14	0.10
Granisetron	5.42	6.03	−0.61
Imipramine	5.47	5.06	0.41
Mizolastine	6.45	6.90	−0.45
Perhexiline	5.11	5.33	−0.22
Terfenadine	6.89	7.06	−0.17
Thioridazine	7.45	7.10	0.35
Ziprasidone	6.82	5.98	0.84

[a] Ref. 9 and the references there in.
[b] Ligands omitted from the final model.

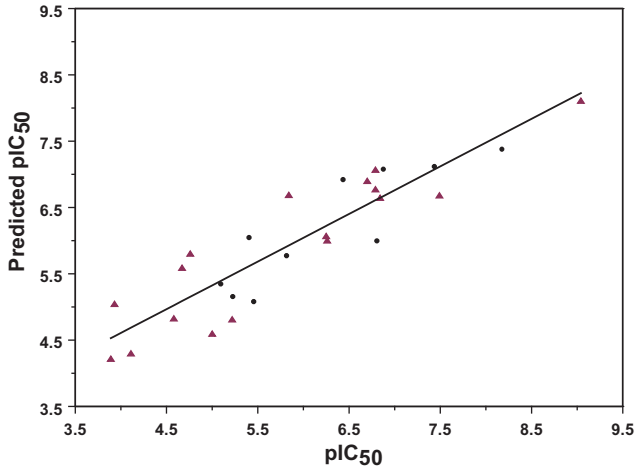

Figure 5. Plot of the experimental versus computed pIC_{50} for the partially open and open state binders with the four possible outlier compounds removed. Red triangles and black circles represent open and partially closed states, respectively. The solid line represents the robust MM fit.

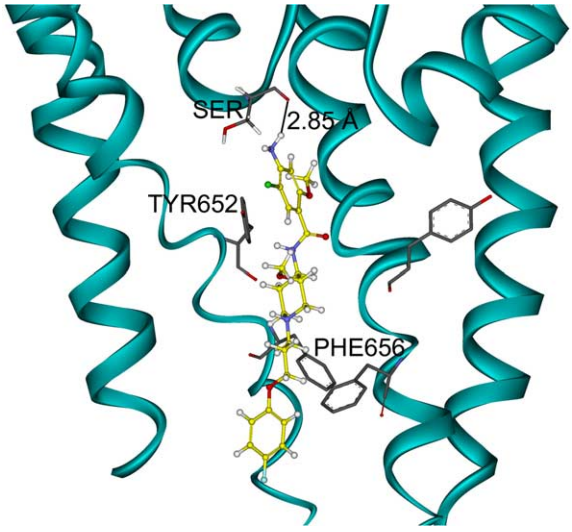

Figure 6. Cisapride docked into the cavity of the partially open state. A close up view of the bound conformer satisfying the general requirements of previously established pharmacophore models.

that the outliers prefer yet another undetermined state that is either more open or closed than the two states considered in this study. A plot of the experimental versus predicted pIC_{50}s for the final set of 27 ligands bound to the open form is shown in Figure 5.

$$pIC_{50_{Combined}} = -0.163(\Delta vdw) + 0.0009(\Delta ele) \qquad (3)$$

The coefficients derived indicate that the primary contribution to the fits arises from the Δvdw term. This observation is in agreement with a recent study by Fernandez et al. where they investigated the binding affinity (log (fold change in IC_{50})) of MK-499, Cisapride and Terfenadine to the wild type and a number of mutants of hERG.[8] They found that one of the best predictors of affinity to a given hERG channel mutant was the hydrophobicity of the pore residue PHE656 and the presence of an aromatic group at TYR652.[8]

Inspection of the binding modes of the ligands docked into the channel shows general agreement with experimental mutation studies and established pharmacophore models. A representative case, shown in Figure 6, is the binding mode of cisapride. The model fits the requirements of a hydrophobic group close to Tyr652, a basic nitrogen in the center of the channel, and a hydrophobic group at the bottom interacting with Phe656. This consistency with the mutational data provides further evidence that the methodology is correctly picking the ligand bound poses. The ability to predict the correct binding mode is important especially when one considers the need for tools to guide synthesis of less potent binders for hERG.

In conclusion, we have developed a two-state hERG binding affinity model that is able to reproduce the pIC_{50} values of a wide range of ligands for the hERG K^+ channel and, results in docked poses that are consistent with published mutation studies. This was not the case for the simple one state model and thus highlights the need for modeling techniques that can capture the flexibility of the hERG K^+ channel.

The ability to predict hERG binding affinities, and probable binding modes for putative ligands to the hERG channel provides a powerful new tool for designing new pharmaceuticals with reduced cardiovascular liability due to hERG. This general approach also provides a new theoretical framework for examining the relationship between ligand binding to hERG and the state of the ion channel.

Acknowledgements

R.R. thanks the Johnson & Johnson Corporate Office of Science and Technology for an Excellence in Science postdoctoral fellowship. We also thank Professor Michael Sanguinetti for helpful discussions.

References and notes

1. Vandenberg, J. I.; Walker, B. D.; Campbell, T. J. *Trends Pharmacol. Sci.* **2001**, *22*, 240.
2. Pearlstein, R. A.; Vaz, R.; Rampe, D. *J. Med. Chem.* **2003**, *46*, 2017.
3. Fermini, B.; Fossa, A. A. *Nat. Rev.* **2003**, *2*, 439.
4. Mitcheson, J. S.; Chen, J.; Lin, M.; Culberson, C.; Sanguinetti, M. C. *Proc. Natl. Acad. Sci. U.S.A.* **2000**, *97*, 12329.
5. Kamiya, K.; Mitcheson, J. S.; Yasui, K.; Kodama, I.; Sanguinetti, M. C. *Mol. Pharmacol.* **2001**, *60*, 244.
6. Sanchez-Chapula, J. A.; Navarro-Polanco, R. A.; Culberson, C.; Chen, J.; Sanguinetti, M. C. *J. Biol. Chem.* **2002**, *277*, 23587.
7. Sanchez-Chapula, J. A.; Ferrer, T.; Navarro-Polanco, R. A.; Sanguinetti, M. C. *Mol. Pharmacol.* **2003**, *63*, 1051.
8. Fernandez, D.; Ghanta, A.; Kauffman, G. W.; Sanguinetti, M. C. *J. Biol. Chem.* **2004**, *279*, 10120.
9. Cavalli, A.; Poluzzi, E.; De Ponti, F.; Recanatini, M. *J. Med. Chem.* **2002**, *45*, 3844.
10. Pearlstein, R. A.; Vaz, R. J.; Kang, J.; Chen, X.; Preobrazhenskaya, M.; Shchekotihin, A. E.; Korolev, A. M.; Lysenkova, L. N.; Miroshinkova, O. L.; Hendrix, J.; Rampe, D. *Bioorg. Med. Chem. Lett.* **2003**, *13*, 1829.
11. Keserü, G. M. *Bioorg. Med. Chem. Lett.* **2003**, *13*, 2773.
12. Zhou, Y.; Morais-Cabral, J. H.; Kaufman, A.; MacKinnon, R. *Nature* **2001**, *414*, 43.
13. Prime, 1.0 ed.; Schrodinger, Inc.
14. Jiang, Y.; Lee, A.; Chen, J.; Ruta, V.; Cadene, M.; Chait, B. T.; MacKinnon, R. *Nature* **2003**, *423*, 33.
15. Jiang, Y.; Lee, A.; Chen, J.; Cadene, M.; Chait, B. T.; MacKinnon, R. *Nature* **2002**, *417*, 523.
16. Brooks, B.; Karplus, M. *J. Comput. Chem.* **1983**, *4*, 187.
17. MacKerell, A.; Bashford, D.; Bellot, M.; Dunbrack, R.; Evanseck, J. D.; Feild, M.; Gao, J.; Guo, H.; Ha, S.; Joseph, D.; Kuchnir, L.; Kuczera, K.; Lau, F.; Mattos, C.; Minchnick, S.; Ngo, T.; Nguyen, D.; Prodhom, B.; Reiher, W. E.; Roux, B.; Schlenkrich, M.; Smith, J.; Stote, R.; Strub, J.; Watanabe, M.; Wiokiewicz-Kuczera, J.; Yin, D.; Karplus, M. *J. Phys. Chem. B* **1998**, *102*, 3586.
18. Maestro, 6.0 ed.; Schrodinger, Inc.
19. Halgren, T. A.; Murphy, R. B.; Friesner, R. A.; Beard, H. S.; Frye, L. L.; Pollard, W. T.; Banks, J. L. *J. Med. Chem.* **2004**, *47*, 1750.
20. Jorgensen, W. L.; Tirado-Rives, J. *J. Am. Chem. Soc.* **1988**, *110*, 1657.
21. Jorgensen, W. L.; Maxwell, D. S.; Tirado-Rives, J. *J. Am. Chem. Soc.* **1997**, *119*, 11225.
22. Qui, D.; Shenkin, P. S.; Hollinger, F. P.; Still, C. W. *J. Phys. Chem. A* **1997**, *101*, 3005.
23. S-Plus, 6.0 ed.; Insightful Corp.